

## Shear-induced permeation and fusion of lipid vesicles

Anne-Laure Bernard<sup>a</sup>, Marie-Alice Guedeau-Boudeville<sup>a,\*</sup>, Valérie Marchi-Artzner<sup>b,1</sup>,  
Thadeus Gulik-Krzywicki<sup>c</sup>, Jean-Marc di Meglio<sup>d</sup>, Ludovic Jullien<sup>e</sup>

<sup>a</sup> *Laboratoire de Physique de la Matière Condensée (CNRS UMR 7125) and Matière et Systèmes Complexes (CNRS FR 2438), Collège de France, 11 Place Marcelin Berthelot, 75231 Paris Cedex 05, France*

<sup>b</sup> *Laboratoire de Chimie des Interactions Moléculaires (CNRS UPR 285), Collège de France, 11 Place Marcelin Berthelot, 75231 Paris Cedex 05, France*

<sup>c</sup> *Centre de Génétique Moléculaire (CNRS UPR 2167), Bât. 26, avenue de la Terrasse, 91198 Gif sur Yvette Cedex, France*

<sup>d</sup> *Laboratoire de Biorhéologie et d'Hydrodynamique Physico-chimique (CNRS UMR 7057) and Matière et Systèmes Complexes (CNRS FR 2438), Université Denis Diderot, 2 place Jussieu Case courrier 7056, 75251 Paris Cedex 05, France*

<sup>e</sup> *Département de Chimie (CNRS UMR 8640), École Normale Supérieure, 24 rue Lhomond, 75231 Paris Cedex 05, France*

Received 2 August 2004; accepted 1 December 2004

Available online 25 April 2005

### Abstract

This paper introduces a novel approach to controlling membrane permeability in free unilamellar vesicles using shearing in the presence of a detergent with a large head-group to tune pore formation. Such shear-induced permeation could offer a simple means of postencapsulating bioactive molecules to prepare vesicle vectors for drug delivery. Using UV absorption, fluorescence emission, dynamic light scattering, and electron microscopy, we investigated the membrane permeability and the morphology of unilamellar lipid vesicles (diameter in the range 50–400 nm) subjected to a shear stress in the presence of a small amount of nonionic surfactant (Brij 76). Shear-induced leakage and fusion events were observed. We analyzed the significance of the vesicle size, the shear rate, and the surfactant-to-lipid ratio for the observed phenomena. The present approach is evaluated for postloading of preformed vesicles.

© 2004 Elsevier Inc. All rights reserved.

**Keywords:** Vesicle; Shearing; Permeation; Surfactant; Fusion; Encapsulation

### 1. Introduction

Chemical agents (addition of solvent, surfactant, or salt modifying the membrane properties, chemical degradation

of the lipids) and physical actions (change of temperature, exposure to UV, osmotic shock) can be used to stress vesicles [1–10]. Among physical sources of stress, shearing exhibits especially attractive features such as tunability and selectivity of action for encapsulating fragile objects such as drug molecules. Shearing found versatile applications for vesicle preparation: large unilamellar vesicles (LUV, diameter 100 to 400 nm) are commonly produced by extrusion and the so-called onion vesicles can be obtained from lamellar phases of monocationic surfactants by shearing in a Couette viscometer [11].

Shearing can also be a strategy for delivering hydrophilic molecules trapped inside vesicles [12–16]. In a first attempt, bilayer permeability in giant unilamellar vesicles (GUV, diameter 1 to 100  $\mu\text{m}$ ) was induced by spreading them onto charged rough surfaces of sporopollenins [13]. We subsequently analyzed the spreading-induced permeability of

*Abbreviations:* ANTS, aminonaphthalene-3,6,8-trisulfonic acid; Brij 76, polyoxyethylene (10) stearyl ether; Brij 700, polyoxyethylene (100) stearyl ether; DLS, dynamic light scattering; DPX, *N,N*-*p*-xylylene-bis(pyridinium bromide); EDTA, ethylenediamine tetraacetate; EPC, egg phosphatidylcholine; GUV, giant unilamellar vesicle; LUV, large unilamellar vesicle; SUV, small unilamellar vesicle; TES, *N*-tris[hydroxymethyl]methyl-2-aminoethanesulfonic acid; Tris buffer, 2-amino-2-(hydroxymethyl) 1,3-propanediol.

\* Corresponding author.

*E-mail address:* [marie-alice.guedeau@college-de-france.fr](mailto:marie-alice.guedeau@college-de-france.fr)

(M.-A. Guedeau-Boudeville).

<sup>1</sup> Present address: SESO (CNRS UMR 6510), Université de Rennes I, 35042 Rennes Cedex, France.

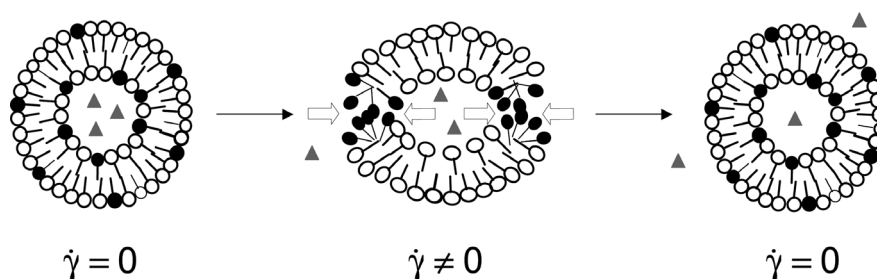


Fig. 1. Schematic diagram of the strategy to induce leakage of vesicles by shearing. Upon shearing, the evenly distributed detergent bearing a large head group partially segregates within the bilayer. This phenomenon promotes the formation of pores favoring exchanges of aqueous solution between the internal and external vesicle pools. Lipid distribution relaxes once the shear stress is stopped.

GUV electrostatically interacting with smooth or decorated planar surfaces [15,16]. In particular, we showed that permeation was governed by pore formation that specifically occurred in heterogeneous domains of the lipid bilayer [17]. The latter observation suggested to us a novel approach to controlling membrane permeability in free vesicles of diameter smaller than that of GUV by using shearing to tune pore formation. Practically, small vesicles are used in many cosmetic or pharmaceutical products (topical, parenteral, oral, inhalation delivery), and control over delivery through shearing effects during application (spreading on skin, shear in blood vessels, etc.) could be useful.

In relation to theoretical works [18], we suggest applying shear stress to deform vesicles made of two components, a lipid matrix (EPC for instance) and a detergent bearing a large head group. The predicted ellipsoidal shape should sterically favor concentration of the detergent at the poles of the deformed vesicles. This phenomenon could lower the local membrane tension and correspondingly determine the pore formation and the leakage of the internal contents (Fig. 1). Indeed, it has already been shown that the presence of detergent favors the formation of pores of critical radius  $r = \gamma/\sigma$ ,  $\gamma$  being the line tension of the pore and  $\sigma$  the membrane tension [19].

In order to determine if the vesicle shape is affected by shear, one introduces the capillary number  $C_a = \Sigma_{\text{stress}}/P_{\text{Laplace}}$ . The latter compares the strength of the shear stress  $\Sigma_{\text{stress}}$  that tends to stretch the vesicle to the Laplace pressure  $P_{\text{Laplace}}$  that tends to restore its spherical shape. The vesicle shape is significantly affected by shear as soon as  $C_a > 1$ . Estimating the membrane tension as  $\Sigma = K_c/R^2$ ,  $C_a$  is written

$$C_a = \frac{\Sigma_{\text{stress}}}{P_{\text{Laplace}}} = \frac{\eta \dot{\gamma} R^3}{K_c}, \quad (1)$$

where  $K_c$ ,  $R$ ,  $\eta$ , and  $\dot{\gamma}$  respectively designate the rigidity constant, the vesicle radius, the solution viscosity, and the shear rate. Taking  $R = 200$  nm,  $\eta = 10^{-3}$  Pa·s, and  $K_c = 10k_B T$  [20], one has  $C_a > 1$  at room temperature as soon as  $\dot{\gamma} > 5000$  s $^{-1}$ . Such numbers are compatible with using large unilamellar vesicles (LUV) and spreading on skin (shear rate  $\sim 1000$  s $^{-1}$ ) [21], shearing in blood capil-

lary vessels (shear rates  $\sim 100$ – $1000$  s $^{-1}$ ) [22,23], or shearing through the nozzle of a hair spray aerosol (shear rate  $\sim 10,000$  s $^{-1}$ ) [24].

The present paper reports on our first results related to the strategy exposed above. It is organized as follows. In a first part, we report on a new permeability test relying on UV–vis absorption spectroscopy that was designed for in situ observation in the transparent Couette viscometer used to induce shearing. The latter test is used to evidence that a shearing stress on the mixed lipid bilayer of EPC:detergent vesicles in the range 50–400 nm induces leakage of water-soluble species through the membrane. Then we analyze the shear effects on the vesicle morphology by complementary techniques such as electron microscopy, dynamic light scattering, and fluorescence emission. The electron microscopy analysis reveals a mechanism more complex than simple leakage leading to vesicle fusion. So we use a fluorescence test after the shear process in order to evaluate the competition between leakage and fusion during the shearing of the vesicles. It was previously reported that the shearing of a lamellar phase creates onions and simultaneously permits encapsulation of materials [25]. Here we consider the postencapsulation of external molecules inside already formed unilamellar vesicles by shearing. The discussion proposes a mechanism that is analyzed in relation to the experimental results and to the expected shearing effects.

## 2. Materials and methods

### 2.1. Materials

ANTS and DPX were obtained from Molecular Probes. Plasmocorinth, EDTA, EPC, Brij 76, and all other chemical compounds were obtained from Sigma-Aldrich, France. Prepacked PD 10 columns (Sephadex G-25M) were obtained from Amersham Biosciences, Sweden. Dialysis membrane (Spectra/Por 4, molecular weight cutoff 12,000–14,000) was obtained from Merck-Eurolab, France. Extrusion membrane (Whatman) was obtained from VWR International, France.

## 2.2. Preparation of vesicle suspensions

Lipid concentration was calculated from the initial amount of lipid used for vesicle preparation and the final aqueous volume. To avoid bursting because of osmotic shocks during exchanges of aqueous solutions in vesicular media, osmolarities were adjusted with buffer or glucose and were measured with a cryoscopic osmometer (Roebbling apparatus).

SUV were prepared by ultrasonication with a 2.5-mm-diameter disruptor tip mounted on a Branson Sonifier (cell disruptor B-30 manufactured by the Branson Sonic Power Company, USA), used in the continuous mode with output level 2 out of 10. A lipid film resulting from evaporating a chloroform solution of EPC under vacuum at room temperature was hydrated with the appropriate solution in a warm bath (40 °C). After 15 min of ultrasonication in an ice bath to avoid any detrimental action of the generated heat, the external solution was exchanged by submitting the vesicles to several dialyses against an isoosmolar solution. After dialysis, the final lipid concentration typically ranges from 40 to 70 mM depending on the preparation.

LUV were prepared by extrusion [26]. An EPC film was hydrated at room temperature using the appropriate solution. The lamellar suspension was submitted to five freeze–thaw cycles using liquid nitrogen and water at 20 °C before being extruded 10 times through a track-etched polycarbonate membrane (100-, 200-, 400-nm pores; Whatman) at 45 °C. The exchange of the vesicle external medium was performed by gel exclusion chromatography on a prepacked Sephadex G-10 column (Pharmacia) by elution with an isoosmolar solution.

## 2.3. Solutions to evaluate shear-induced leakage

Internal vesicle compartments: 5 mM Plasmocorinth [27], 5 mM MgCl<sub>2</sub>, 50 mM Tris pH 8 (osmolarity: 113 mOsmol). External vesicle compartments: 12 mM EDTA, 50 mM Tris pH 8 (osmolarity: 113 mOsmol).

## 2.4. Solutions to evaluate shear-induced fusion [28,29]

Internal vesicle compartments: either (i) 25 mM ANTS, 10 mM TES pH 7.4, 120 mM glucose (ANTS LUV 100); (ii) 90 mM DPX, 10 mM TES pH 7.4 (DPX LUV 100); or (iii) 12.5 mM ANTS, 45 mM DPX, 10 mM TES pH 7.4 (ANTS/DPX LUV 100). External vesicle compartments: 10 mM TES pH 7.4, 200 mM glucose. The osmolarities of the three solutions were adjusted with glucose to 216 mOsm.

## 2.5. Couette cell

The Couette cell (CAPLIM, Bordeaux, France; see Fig. 1S in Supplementary Material) consists of one inner stator and three different-sized outer rotors, allowing gaps of 0.3, 0.5, and 1 mm for shear rates up to 20,000 s<sup>-1</sup>. It is

made of transparent polymethylmethacrylate (PMMA) that allows spectroscopic measurements in situ. The temperature of the sheared solution in the Couette was calibrated as a function of the shear rate by recording the absorbance of a Plasmocorinth solution whose dependence on temperature was independently measured in a cuvette.

## 2.6. Photophysical experiments

Absorption spectra were recorded with a Cary 217 Varian spectrometer (Couette experiments) or a Beckman DU 640 spectrometer (cuvette experiments). Fluorescence spectra were recorded with a SPEX Fluoromax fluorimeter. Emission spectra were recorded under a monochromatic excitation wavelength of  $\lambda_{\text{exc}} = 320$  nm. Temperature was fixed at 20 °C with a circulating water bath during these experiments.

## 2.7. Freeze-fracture transmission electron microscopy

Samples of LUV were studied before and after shearing. In order to achieve the best preservation of the sample structure upon cryofixation, glycerol (33% v/v) was added into the external media. A layer of the sample 20–30  $\mu\text{m}$  thick was deposited on a thin copper holder and then rapidly quenched in liquid propane. The frozen samples were fractured under vacuum ( $10^{-7}$  Torr) with a liquid-nitrogen-cooled knife inside a freeze-etching unit (Balzers 301). The replication was done using unidirectional shadowing with Pt–C at an angle of 35°. The mean thickness of the metal deposit was 1.0–1.5 nm. The replicas were washed with organic solvents and distilled water and then observed with an electron microscope (Philips EM 410). The contrast in images is related to the depth fluctuations of the metal deposit. The mean diameters were measured on electron micrographs and are corrected by a factor of  $4/\pi$  to account for the random cleavage of the vesicle by cryofracture.

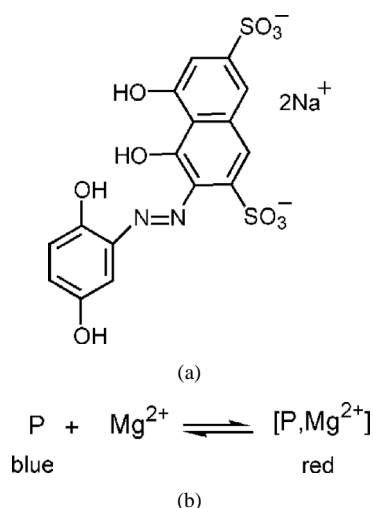
## 2.8. Dynamic light scattering (DLS)

All the vesicle samples at lipid concentration 0.1–0.5 mM were filtered (Nucleopore, pore size 0.25  $\mu\text{m}$ ) before experiments. The dynamic light-scattering measurements were carried out on a 4700/PCS100 Malvern apparatus at 50° to take into account the largest particles using an Ar laser (514.5 nm). Correlation functions were analyzed by the cumulant method to estimate the hydrodynamic diameter of the vesicles.

## 3. Results

### 3.1. Set-up of a test for direct observation of shearing-induced vesicle leakage in a Couette cell

We have first looked for a technique to study the bilayer permeability possibly induced during vesicle shearing. The



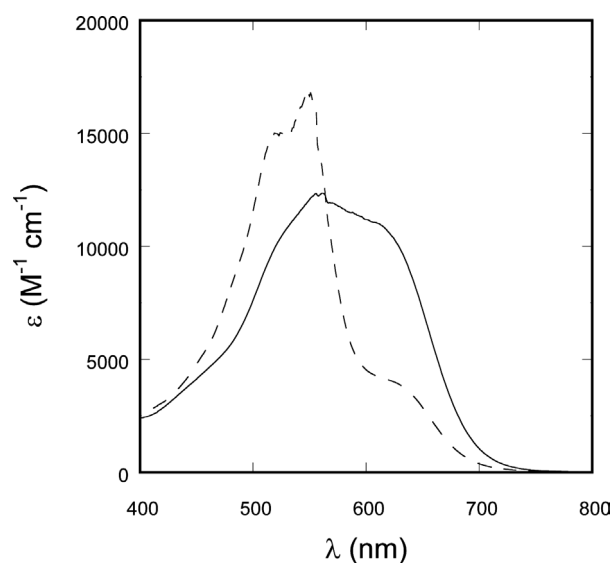
Scheme 1. (a) Molecular structure of Plasmocorinth B (P); (b) complexation process occurring between Plasmocorinth B and the magnesium (II) cation.

classical test based on calcein [30] was first envisaged. Unfortunately we observed that the vesicles and the fluorescent dye adsorbed onto the walls of the Couette cell at the relevant concentrations; in addition, the geometry of the Couette cell was not favorable to recording fluorescence emission spectra. Thus we designed a new permeability test based on UV–vis absorption and relying on larger concentrations (typically 1 mM in dye and 10 mM in lipid) to decrease the significance of nonspecific adsorption.

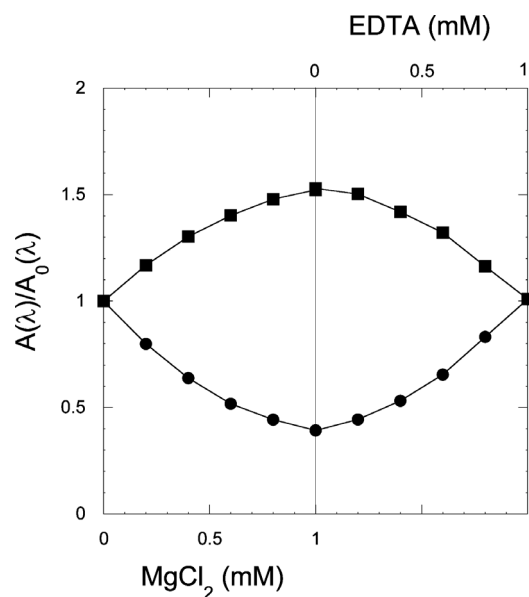
The principle of this new permeability test is similar to that of the calcein one: when the contents of the internal and external vesicular compartments come into contact, the reaction occurring between a cation and a ligand initially separated induces a major change of the spectroscopic properties of the ligand. We chose Plasmocorinth B (denoted P) as a ligand (Scheme 1).

This azo dye gives a 1:1 complex with  $Mg^{2+}$  and correspondingly exhibits a significant change of its absorption visible-spectrum in a favorable range of wavelengths to facilitate correction from light scattering induced by vesicles (Fig. 2a) [27]. The symmetry of the curves giving relative absorbances at 520 and 620 nm upon successive additions of  $Mg^{2+}$  and EDTA (Fig. 2b) suggests that P can be regenerated from P:Mg(II) due to formation of the more stable 1:1 EDTA:Mg(II) complex. The low curvatures of the corresponding curves indicate that complexation of  $Mg^{2+}$  by P or displacement of P:Mg(II) after EDTA addition are essentially complete under the present experimental conditions.

These properties, observed in solution, were then used in the case of our vesicular systems. The internal vesicle compartment is loaded with the P:Mg(II) complex and the external compartment contains EDTA; the latter  $Mg^{2+}$  ligand is added (i) to favor displacement of  $Mg^{2+}$  from the P:Mg(II) complex and (ii) to avoid any interaction between the divalent cation and the polar head groups of the vesicle lipids. Before contact between the internal and external pools, the vesicle suspension is red, whereas it becomes blue after per-



(a)



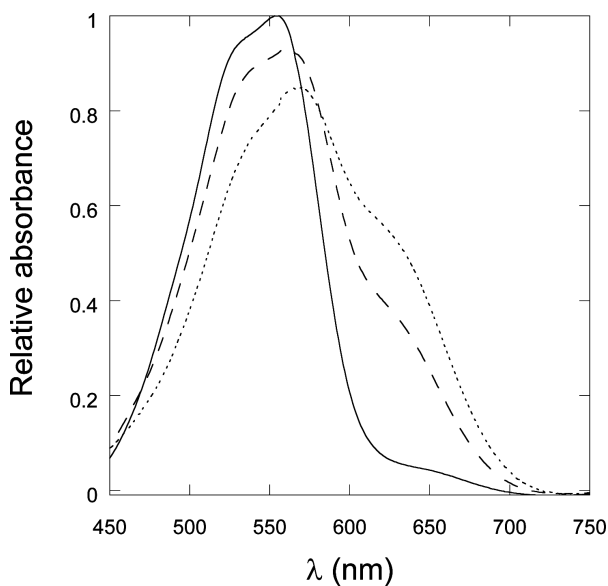
(b)

Fig. 2. (a) Evolution of the extinction coefficient  $\varepsilon$  vs the wavelength  $\lambda$  of solutions of P (solid line) and of the P:Mg(II) complex (dashed line) in 50 mM Tris pH 8: the formation of the 1:1 complex with  $Mg^{2+}$  induces a blue shift of the P absorption spectrum. (b) Evolution of the relative absorbance at 520 nm (squares) and 620 nm (circles) during titration of 1 mM P with  $MgCl_2$  up to 1 mM in  $MgCl_2$ , followed by titration with EDTA, in Tris 50 mM pH 8.

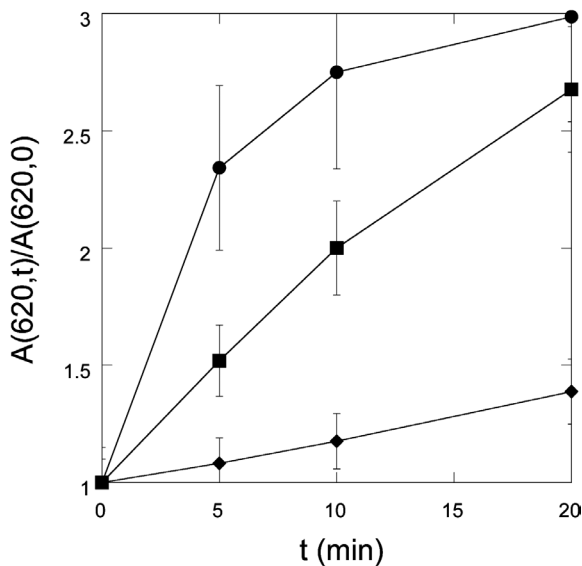
meation through the lipid bilayer. The corresponding alteration of the absorption spectrum of the vesicle suspension can be used to follow the exchange of the aqueous solution between the vesicle pools.

### 3.2. Shear-induced leakage in EPC vesicles

Four different batches of EPC vesicles containing the P:Mg(II) complex (respectively EDTA) in their internal (respectively external) compartments were prepared using either ultrasonication or extrusion through carbonate filters



(a)



(b)

Fig. 3. (a) Evolution of the relative absorbance of LUV 100 ( $C_{lip} = 7.5$  mM) suspension in the presence of 1% (mol/mol) Brij 76 at shear rate  $10,000\text{ s}^{-1}$  as a function of shear time (0 min: solid line; 20 min: dashed line) at room temperature. In a purpose of comparison, the relative absorbance after cholate addition leading to vesicle disruption is also displayed (dotted line). (b) Evolution of the relative absorbance at 620 nm as a function of shear time at room temperature in LUV 100 suspension at different concentrations in Brij 76: 0% (diamonds), 0.1% mol/mol (squares), 1% mol/mol (circles) (shear rate =  $10,000\text{ s}^{-1}$ ).

with holes of increasing diameter: 100, 200, and 400 nm. The corresponding suspensions of EPC vesicles are respectively designated by SUV, LUV 100, LUV 200, and LUV 400 in the following.

LUV 100 were first submitted to shearing at  $10,000\text{ s}^{-1}$  at room temperature [31] in the Couette viscometer. As displayed in Fig. 3b, only a weak leakage was observed after 20 min. Then we added to the vesicle suspension a

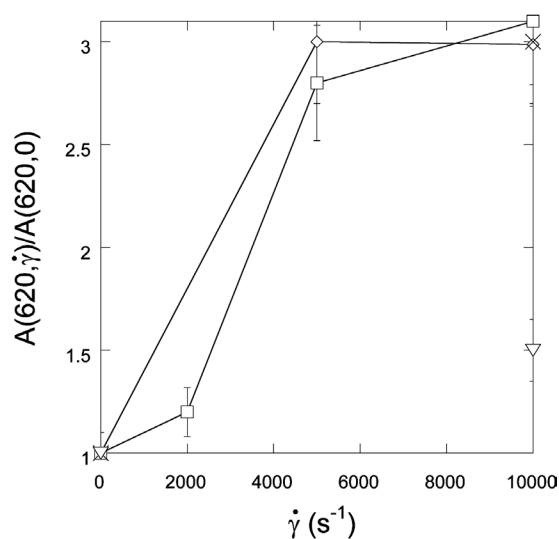


Fig. 4. Evolution of the relative absorbance at 620 nm as a function of shear rate for different suspensions of EPC vesicles ( $C_{lip} = 7.5$  mM) in the presence of 1% (mol/mol) Brij 76 after 20 min of shearing at room temperature. LUV 100 (diamonds), LUV 200 (squares), LUV 400 (cross), SUV (triangle).

detergent bearing a large head group following the strategy evoked in the Introduction [32]. The study was restricted to Brij 76 ( $C_{18}OE_{10}$ ) which induced the desired phenomenon of permeation under shearing. This detergent was chosen because of its electric neutrality and its favorable partition coefficient between the aqueous solution and the membrane [33]. This method could be extended to other detergents presenting the same properties. Brij 76 was added at 0.1 or 1% (mol/mol) with respect to EPC in LUV 100 ( $C_{lip} = 7.5$  mM). Such detergent concentrations (respectively 0.0075 and 0.075 mM) are above its critical micellar concentration ( $cmc = 0.003$  mM at  $25^\circ\text{C}$ ) [34]. Without shearing, no bilayer permeation occurred up to 1% (mol/mol) in Brij 76: we did not observe any evolution of the vesicle suspension at the day timescale. In contrast, bilayer permeability dramatically increased under shear at  $10,000\text{ s}^{-1}$  (Figs. 3a and 3b). The extent of permeation increases at short times and then saturates: at 1% (mol/mol) in Brij 76, the plateau is almost reached after 10 min. The same experiments carried out on LUV 200 and LUV 400 led to similar results. Fig. 3b shows that increasing detergent concentration increases the rate of permeation.

The significance of vesicle size was studied for a given concentration of Brij 76 at different shear rates at room temperature. Fig. 4 displays the extent of permeation induced by shearing in LUV 100 and LUV 200 in the presence of 1% (mol/mol) Brij 76 after 20 min at 2000, 5000, and  $10,000\text{ s}^{-1}$ . The permeation extents in SUV and LUV 400 in the presence of 1% (mol/mol) Brij 76 after 20 min at  $10,000\text{ s}^{-1}$  are also shown in Fig. 4. One notices that the extent of permeation increases with the shear rate but reaches a plateau above  $5,000\text{ s}^{-1}$  for both LUV 100 and LUV 200. In addition, LUV are more sensitive to shearing than the SUV.

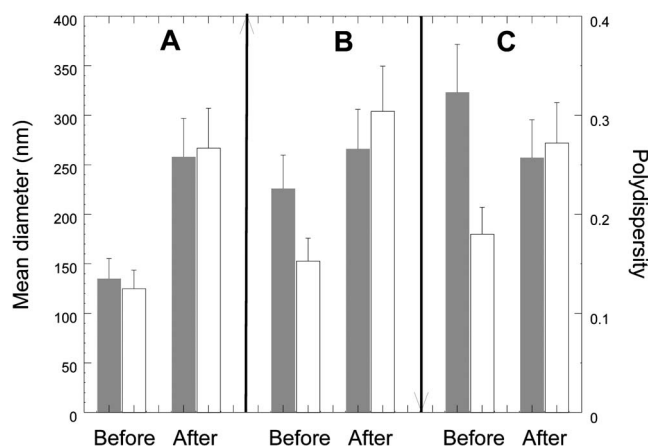


Fig. 5. Mean diameter (gray bars) and polydispersity (white bars) of LUV 100 (A), LUV 200 (B), and LUV 400 (C) before and after shearing at room temperature at  $10,000\text{ s}^{-1}$  for 20 min in the presence of 1% (mol/mol) Brij 76.

### 3.3. Shear-induced fusion in EPC vesicles

Dynamic light scattering (DLS) was used to characterize the vesicle preparations. The diameter of the SUV was found in the 50-nm range. Fig. 5 compares the average diameters and polydispersities [35] of the different LUV samples. The average diameters are in line with the mesh size of the filter used (135, 225, and 325 nm for 100-, 200-, and 400-nm mesh size filters, respectively). As already noted elsewhere [36], the vesicle samples prepared by extrusion on the 100- or 200-nm mesh size filters are less polydisperse than vesicles prepared on the 400-nm mesh size filters. In addition, it is already known that EPC LUV obtained with a 100-nm mesh size filter are more unilamellar than EPC LUV made with a 200-nm mesh size filter, those prepared with the 400-nm mesh size filters being rather multilamellar [26].

Fig. 5 shows that shearing of the LUV in the presence of 1% (mol/mol) Brij 76 at  $10,000\text{ s}^{-1}$  for 20 min at room temperature strongly modifies the size distribution of vesicle suspensions: the average diameter of the LUV 100 and of the LUV 200 is increased, whereas the average diameter of the LUV 400 is decreased. Big objects were formed from the originally “small” LUV 100 and LUV 200, whereas some of the largest vesicles from the LUV 400 preparation broke. Moreover, the polydispersity increased with shearing, whatever the initial diameter of the vesicles. In fact, it seems that the EPC vesicles reached a similar state after shearing independent of their initial size distribution (average diameter around 260 nm and polydispersity around 0.3 after 20 min of shearing at  $10,000\text{ s}^{-1}$ ).

With a view to determining if the created objects were lipid aggregates or fused vesicles, the sheared samples were observed by freeze-fracture electron microscopy. Figs. 6a and 6b respectively display LUV 100 before and after shearing for 20 min at  $10,000\text{ s}^{-1}$  in the presence of 1% mol/mol Brij 76 at room temperature. Fig. 6b does not exhibit any vesicle aggregate. Moreover, conservation of the surface of

the lipid bilayer suggests that vesicle breakage leading to lipid aggregates is a minor phenomenon if present. In contrast, Fig. 6b confirms that fusion of vesicles does occur upon shearing: it evidences the presence of very large unilamellar vesicles with diameters up to  $1\text{ }\mu\text{m}$ . In contrast, fusion was not observed after shearing the LUV 100 nm in the absence of Brij 76.

### 3.4. During shearing

To evaluate the competition between the processes of leakage and fusion during shearing, we turned to the fluorimetric ANTS/DPX fusion test [28,29]. Collisional quenching is responsible for extinction of ANTS fluorescence by DPX. At too low a concentration in a 1:1 (mol/mol) ANTS:DPX mixture, the fluorescence of ANTS is visible. In contrast, the ANTS fluorescence is quenched at large concentrations. We recorded the emission spectra from 2 mM ANTS/DPX LUV 100, and from a 1:1 (mol/mol) mixture of 2 mM ANTS LUV 100 and 2 mM DPX LUV 100 (see Section 2) before and after 20 min of shearing at  $10,000\text{ s}^{-1}$  in the presence of 1% (mol/mol) Brij 76 at room temperature ( $\lambda_{\text{exc}} = 320\text{ nm}$ ).

The initially low fluorescence emission from 2 mM ANTS/DPX LUV 100 in the presence of 1% (mol/mol) Brij 76 increased by a factor of 10 after shearing for 20 min at  $10,000\text{ s}^{-1}$ . This observation confirmed the results from the permeation test: a shearing-induced leakage through the bilayer dilutes the internal 1:1 ANTS:DPX solution and the quenching of ANTS by DPX becomes less efficient.

The initially large fluorescence emission from a 1:1 (mol/mol) mixture of 2 mM ANTS LUV 100 and 2 mM DPX LUV 100 decreased to 2/3 of its original value after shearing for 20 min at  $10,000\text{ s}^{-1}$  at room temperature. As a control experiment no change in fluorescence was observed without shearing for several hours. Under the concentrations used, 100% leakage upon shearing would hardly alter the fluorescence intensity; dilution of ANTS can only increase its quantum yield of fluorescence and essentially no quenching by DPX is expected after 100% leakage. In contrast, 100% of fusion of the internal compartment would lead to observation of a fluorescence intensity similar to that from the ANTS/DPX LUV 100. Thus the observed decrease in emission intensity clearly shows that fusion of the aqueous compartments is a faster process than leakage during shearing.

### 3.5. Vesicle postloading by shearing

We finally undertook to postencapsulate molecules inside vesicles under shear. In fact, this could be an interesting alternative when fragile or expensive molecules are concerned, since vesicle preparation and encapsulation would be dissociated. Indeed, the Brij 76 detergent could be removed in a subsequent step either by dialysis or using adsorption on latex beads [37].

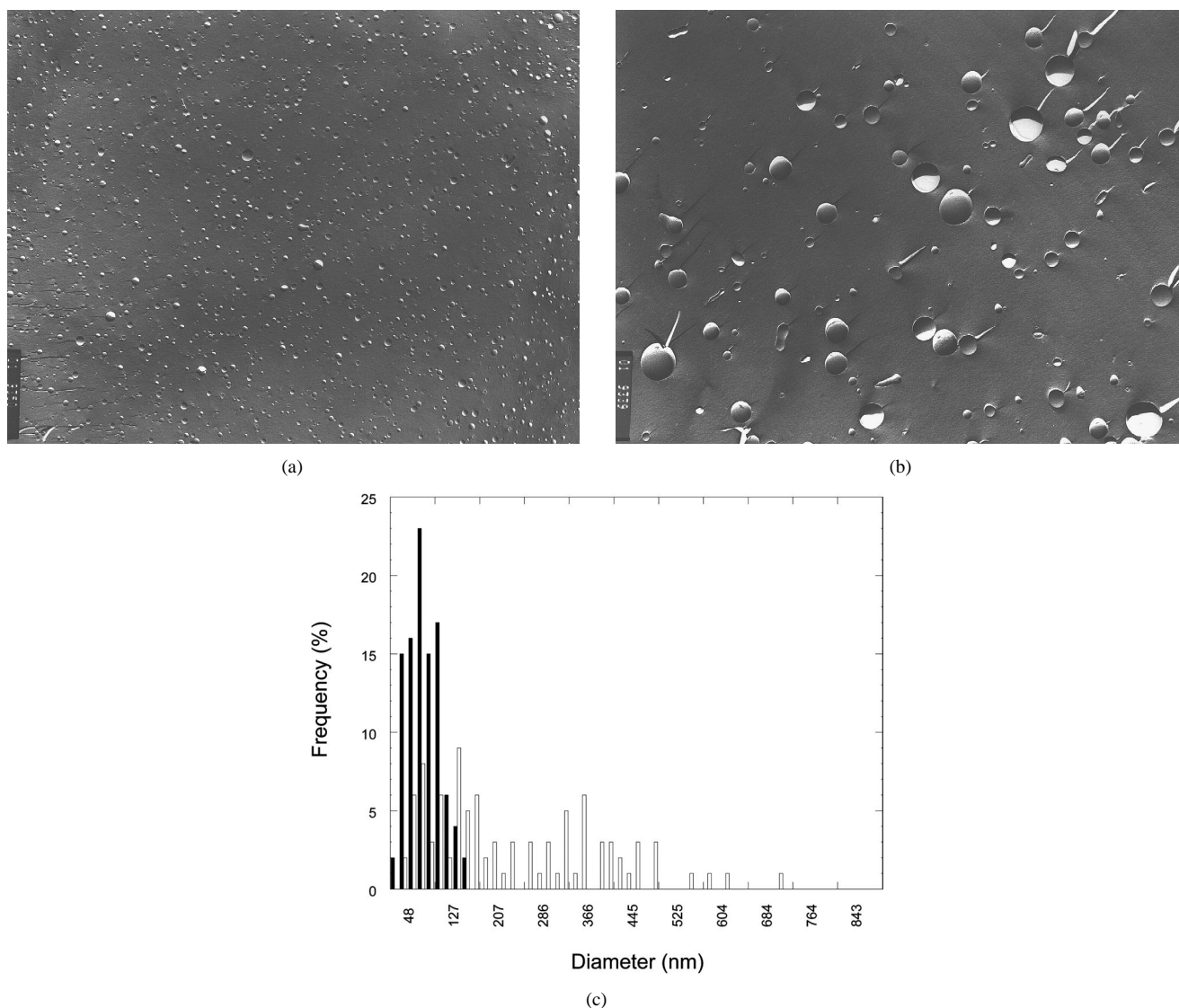


Fig. 6. Freeze-fracture electron microscopy pictures of LUV 100 before (a) and after (b) shearing for 20 min at  $10,000 \text{ s}^{-1}$  in the presence of 1% mol/mol Brij 76 at room temperature (black bar =  $1.5 \mu\text{m}$ ); (c) corresponding size histogram of the same samples before (black bars) and after shearing (white bars). These histograms were obtained from analysis of 220 vesicles in each picture.

EPC LUV 100 ( $C_{\text{lip}} = 6.6 \text{ mM}$ ) prepared without calcein, containing only 50 mM Tris at pH 8 in the internal medium, were sheared in the presence of 1% (mol/mol) Brij 76 in a solution containing  $0.9 \mu\text{M}$  calcein 50 mM Tris pH 8 (external medium) for 20 min at  $10,000 \text{ s}^{-1}$  at room temperature. Then the calcein remaining in the external medium was removed by two successive chromatographies on gel exclusion columns with 50 mM Tris pH 8 as elution solution. The fluorescence emission of these filtered vesicles only originating from the calcein entrapped inside the vesicles after shear was identical to the fluorescence emission from a  $0.02 \mu\text{M}$  calcein solution. It corresponds to the fluorescence of the internal volume of the vesicles filled with the  $0.9 \mu\text{M}$  calcein external solution during the shear. This value (about 2% of the starting external medium concentration) satisfactorily compares with the theoretical internal volume for EPC LUV 100 ( $C_{\text{lip}} = 6.6 \text{ mM}$ ): 2% of the total volume, assuming a

polar head surface per lipid of  $70 \text{ \AA}^2$  [1,38]. Thus  $0.9 \mu\text{M}$  calcein penetrates inside the vesicles during shearing up to equilibration between the concentrations of calcein inside and outside the vesicles. Therefore, the postloading of the vesicles by shearing was only limited by the volume fraction of their internal compartment.

#### 4. Discussion

The present series of experiments evidences the significance of a shear on the behavior of EPC vesicles. Fusion and leakage events were observed in the presence of Brij 76 depending on diverse factors such as average vesicle size, molar fraction of the detergent, and shear rate. Fig. 7 displays a tentative mechanism to account for our observations.

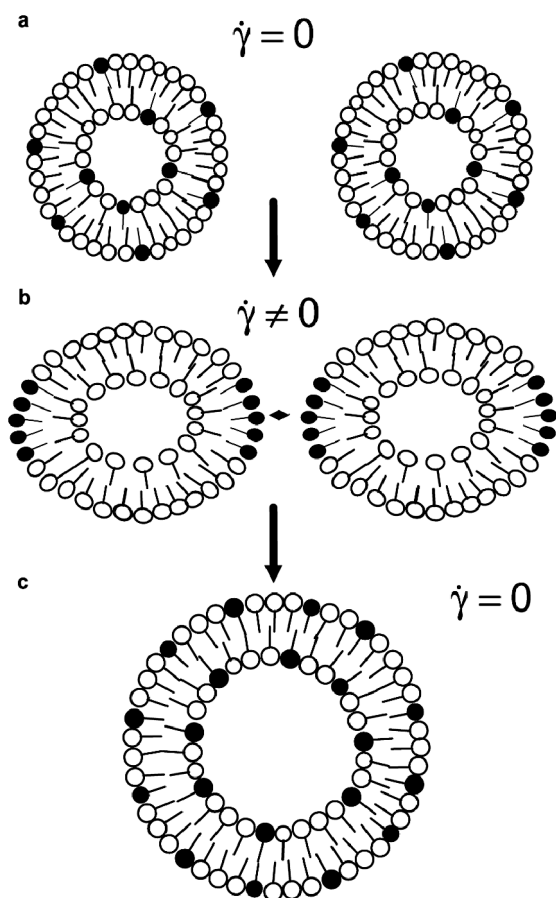


Fig. 7. Schematic diagram of the mechanism governing the shearing-induced fusion and shearing-induced leakage of vesicles. Upon shearing, the Brij 76 molecules partially segregate to accommodate the less-curved positions within the bilayer. This phenomenon promotes the formation of pores favoring leakage. In addition, interaction of vesicles can lead to fusion. In contrast, the largest vesicles are prone to scission.

One first examines the effect of the Brij 76 concentration on the leakage/fusion phenomena. In the absence of detergent, we observed no significant leakage of EPC LUV 100. In the presence of detergent (up to 1% mol/mol to EPC) but without shear, no permeation occurred, as anticipated from the homogeneous distribution of the detergent in the bilayer. In contrast, the analysis relying on the capillary number  $C_a$  defined in the Introduction supports the conclusion that the shape of the largest fraction of the LUV investigated in the present study is significantly affected by shear at the largest examined shear rates; in view of the large spontaneous curvature of Brij 76, shearing here induces segregation of the Brij 76 molecules in the bilayer, which decreases the line tension. Leakage and fusion are facilitated; the more Brij 76 the easier this is.

Fig. 4 shows that the rate of leakage increases with the shear rate until a certain threshold is reached. Two factors play a role here. First shear increases the Brij 76 concentration at the vesicle poles, as already discussed above. In addition, shear increases the collision frequency between vesicles. Indeed, Smoluchowski showed that the kinetics of

coagulation of particles submitted to a shear stress is a law of the second order with a characteristic time  $\tau_{\text{coll}}^{\dot{\gamma}}$  if we consider soft shocks making them stick together [39]:

$$\tau_{\text{coll}}^{\dot{\gamma}} = \frac{3}{32\dot{\gamma}R^3N_0}. \quad (2)$$

$N_0$  is the concentration of vesicles and  $R$  their average radius. By comparison, the characteristic time  $\tau_{\text{coll}}^0$  for collision at rest, determined by the Brownian motion, is

$$\tau_{\text{coll}}^0 = \frac{1}{8\pi DRN_0}, \quad (3)$$

where  $D = k_B T / 6\pi\eta R$  designates the diffusion coefficient of vesicles ( $\eta$  is the external average viscosity). If the adimensional ratio  $\beta = \tau_{\text{coll}}^{\dot{\gamma}} / \tau_{\text{coll}}^0 = k_B T / 8\eta\dot{\gamma}R^3$  is less than 1, vesicle coalescence will rely on shear and not on Brownian motion. In the case of vesicles, the condition  $\beta < 1$  is fulfilled as soon as  $R > 40$  nm (taking  $kT = 4 \times 10^{-21}$  J at room temperature,  $\eta = 10^{-3}$  Pa s, and  $\dot{\gamma} = 10,000$  s $^{-1}$ ). Thus shearing does increase the number of collisions between most vesicles investigated in the present study. The increase of the coalescence rate due to shearing is expected to strongly depend on vesicle size. The phenomenon is much more pronounced for large vesicles.

Eventually vesicle size plays a major role in determining the significance of shearing; the smallest vesicles are less affected by shearing than the largest (see Fig. 4). Indeed, SUV are the vesicles least responsive to shearing. One notices that LUV 100, LUV 200, and LUV 400 behave rather similarly. Explanation of the latter observation probably relies on vesicle multilamellarity. Extrusion is prone to produce a larger fraction of multilamellar vesicles when filters with large holes are used [26]. In the case of multilamellar vesicles, the leakage/fusion mechanism should be less effective than expected for the largest vesicles.

## 5. Summary

This paper demonstrates that shearing considerably affects suspensions of EPC vesicles in the range 50–400 nm at rates beyond 5000 s $^{-1}$  when suitable detergents are added. Shear-induced leakage through lipid bilayers was evidenced with a new permeability test based on UV–vis absorption. Diffusion light scattering and electron microscopy showed that shear can also promote the membrane fusion of the vesicles; whatever the initial size of the vesicles, a same steady state seems to be reached after fusion and scission events respectively involving the smallest and the largest vesicles. The fluorescence ANTS/DPX test demonstrated that fusion occurs faster than leakage upon shearing. Finally, shearing is suggested as an attractive tool for post-loading preformed vesicles.

## Acknowledgments

We thank Hubert Hervet for helpful discussions concerning the Cary spectrometer and the dynamic light scattering measurements and Jean-Claude Dedieu for the electron microscopy measurements.

## Supplementary material

The online version on this article contains additional supplementary material.

Please visit doi:10.1016/j.jcis.2004.12.019.

## References

- [1] D.D. Lasic, *Liposomes: From Physics to Applications*, Elsevier, 1993.
- [2] R.R.C. New, *Liposomes: A Practical Approach*, IRL Press, Oxford/New York/Tokyo, 1990.
- [3] Y. Nagawa, S.L. Regen, *J. Am. Chem. Soc.* 113 (1991) 7237–7240.
- [4] Y. Nagawa, S.L. Regen, *J. Am. Chem. Soc.* 114 (1992) 1668–1672.
- [5] K. Naka, A. Sadownik, S.L. Regen, *J. Am. Chem. Soc.* 114 (1992) 4011–4013.
- [6] Y. Liu, S.L. Regen, *J. Am. Chem. Soc.* 115 (1993) 708–713.
- [7] M. Shibakami, M. Inagaki, S.L. Regen, *J. Am. Chem. Soc.* 119 (1997) 12,354–12,357.
- [8] K. Takiguchi, F. Nomura, T. Inaba, I. Takeda, A. Saitoh, H. Hotani, *Chem. Phys. Chem.* 3 (2002) 571–574.
- [9] R. Blumenthal, M.J. Clague, S.R. Durell, R.M. Eppard, *Chem. Rev.* 103 (2003) 53–70.
- [10] J.C. Bradley, M.-A. Guedeau-Boudeville, G. Jeandeau, J.-M. Lehn, *Langmuir* 13 (1997) 2457–2462.
- [11] O. Diat, D. Roux, F. Nallet, *J. Phys. II Fr.* 3 (1993) 1427–1452.
- [12] M. Dvolaitzky, P.-G. de Gennes, M.-A. Guedeau-Boudeville, L. Jullien, *C. R. Acad. Sci. Paris Sér. II* 316 (1993) 1687–1690.
- [13] M.-A. Guedeau-Boudeville, L. Jullien, J.-M. di Meglio, *Proc. Natl. Acad. Sci. USA* 92 (1995) 9590–9592.
- [14] N. Shahidzadeh, D. Bonn, O. Aguerre-Chariol, J. Meunier, *Phys. Rev. Lett.* 81 (1998) 4268–4271.
- [15] A.-L. Bernard, M.-A. Guedeau-Boudeville, L. Jullien, J.-M. di Meglio, *Langmuir* 16 (2000) 6809–6820.
- [16] A.-L. Bernard, M.-A. Guedeau-Boudeville, O. Sandre, S. Palacin, L. Jullien, J.-M. di Meglio, *Langmuir* 16 (2000) 6801–6808.
- [17] See also F. Brochard-Wyart, P.-G. de Gennes, O. Sandre, *Physica A* 278 (2000) 32–51.
- [18] M. Kraus, W. Wintz, U. Seifert, R. Lipowsky, *Phys. Rev. Lett.* 77 (1996) 3685–3688.
- [19] C. Taupin, M. Dvolaitzky, C. Sauterey, *Biochemistry* 14 (1975) 4771–4775.
- [20] F. Brochard, J.F. Lennon, *J. Phys. Fr.* 36 (11) (1975) 1035–1047.
- [21] J.A. Bouwstra, P.L. Honeywell-Nguyen, *Adv. Drug. Delivery Rev.* 54 (2002) 541–555.
- [22] Y. Leong Yeow, S. Ranil Wickramasinghe, Y.-K. Leong, B. Han, *Biotechnol. Prog.* 18 (2002) 1068–1075.
- [23] Y.C. Fung, *Biomechanics Circulation*, second ed., Springer-Verlag, New York, 1997.
- [24] Estimation for a nebulizer or hairspray aerosol (flow rate  $\sim 1500 \mu\text{l}/\text{min}$ ; nozzle diameter  $\sim 200 \mu\text{m}$ ).
- [25] O. Freund, P. Mahy, J. Amedee, D. Roux, R. Laversanne, *J. Microencapsul.* 17 (2) (2000) 157–168.
- [26] M.J. Hope, M.B. Bally, G. Webb, P.R. Cullis, *Biochim. Biophys. Acta* 812 (1985) 55–65.
- [27] G. Charlot, *Les méthodes de la chimie analytique*, fourth ed., Masson, Paris, 1961.
- [28] N. Düzgünes, T.M. Allen, J. Fedor, D. Papahadjopoulos, *Biochemistry* 26 (1987) 8435–8442.
- [29] V. Marchi-Artzner, T. Gulik-Krzywicki, M.-A. Guedeau-Boudeville, C. Gosse, J.M. Sanderson, J.-C. Dedieu, J.-M. Lehn, *Chem. Phys. Chem.* 2 (2001) 367–376.
- [30] D.A. Kendall, R. McDonald, *Anal. Biochem.* 134 (1983) 26–33.
- [31] See Section 2. No significant difference in permeation rates were observed between 10 and 40 °C for the chosen vesicle suspensions.
- [32] R. Schubert, H. Wolburg, K. Schmidt, H. Roth, *Chem. Phys. Lip.* 58 (1991) 121–129.
- [33] As a comparison, we observed that Brij 700 ( $\text{C}_{18}\text{OE}_{100}$ ) did not induce any permeability during shearing.
- [34] From Sigma Product Information Sheet about Brij detergents.
- [35] The polydispersity coefficient characterizes the polydispersity of the diffusion coefficient but reasonably varies in the same direction as the polydispersity for the diameters. Above 0.3, the polydispersity index is meaningless.
- [36] L.D. Mayer, M.J. Hope, P.R. Cullis, *Biochim. Biophys. Acta* 855 (1986) 223–230.
- [37] J.-L. Rigaud, D. Levy, G. Mosser, O. Lambert, *Eur. Biophys. J.* 27 (1998) 305–319.
- [38] The total internal volume fraction of such vesicle dispersion was evaluated to lie between 1 and 2% by NMR experiments. See V. Marchi-Artzner, L. Jullien, L. Belloni, D. Raison, L. Lacombe, J.M. Lehn, *J. Phys. Chem.* 100 (1996) 13,844–13,856.
- [39] V.G. Levich, *Physicochemical Hydrodynamics*, Prentice–Hall, Englewood Cliffs, NJ, 1962.